Performance prediction of magnetorheological valves under various type of fluid and flux path

Muhammad Hafiz Idris[1], *Saiful Amri* Mazlan[1*], *Ubaidillah* Ubaidillah[2], and *Fitrian* Imaduddin[3]

[1]Malaysia-Japan International Institute of Technology, Universiti Teknologi Malaysia, 54100 Jalan Sultan Yahya Petra, Kuala Lumpur, Malaysia
[2]Mechanical Engineering Department, Faculty of Engineering, Universitas Sebelas Maret. J1 Ir. Sutami 36A, Kentingan, Surakarta, 57126, Central Java, Indonesia
[3]Faculty of Engineering and Technololgy, Multimedia University, Jalan Ayer Keroh Lama, Bukit Beruang, 75450 Melaka, Malaysia

Abstract. Magnetorheological (MR) valve is one of the key components in regulating the control flow of MR fluid flow in MR devices. Due to MR rheological properties enabling magnetic modifications, many MR valve designs have been introduced and are widely utilized in MR devices. The main objective of this article is to compare the pressure drop generated by each types of MR valves. Five different configurations of MR valves were analyzed in this study. To provide a fair comparison, several parameters were fixed; which is the size of the MR valves, gap size, number of coil turns and power consumption. In order to demonstrate the MR valve performance, the pressure drops were calculated based on the mathematical equations derived from MR valve models and the magnetic fields derived from finite element method based software. The results of the simulations were compared to each type of MR valve and, then, discussed.

1 Introduction

Recently, applications and devices utilizing magnetorheological fluids (MRFs) are experiencing a rise due to the property uniqueness of magnetic controllable and fast-response rheological change with the magnetic field. MRF is a type of smart material where the viscosity of the fluid increases when the magnetic field increases[1]. Currently, MRF devices use several modes of operations, and the most commonly used are the valve mode also known as MR valve [2–4]. A conventional MR valve includes an electromagnetic coil to generate the magnetic field intensity. The pressure drop of the MR valve rises with the raising of the magnetic field strength.

The valve dimensions and configurations has been observed to affect the performances of the MR valve. Researchers have developed several studies on the geometrical arrangements, which utilizes the gaps for the fluid flow path known as annular and radial gaps [5]. An annular gap is a flow channel that allows the MRF flows axially in the MR

* Corresponding author: amri.kl@utm.my

valve and the placement of it is parallel to the inlet and outlet of the valve. Meanwhile, for the radial gaps, the fluid flows transversely in a radial manner, forcing the fluid to flow in perpendicular to the inlet and outlet of the valve. These two gap types, annular and radial, are the most commonly and widely used in studies. The applications have been established in the MR devices [6–8]. The progress of the MR valve studies also continues with new types of configurations which are serpentine configuration and meandering configuration [3,9]. The magnetic flux in the design of serpentine MR valve is weaved into the annular gap by alternating the non-magnetic and magnetic materials. While, in meandering configuration, the multiple annular and radial configurations are combined with orifice flow channel, which also extends the flow path of the valve.

One study reported a methodology in configuring and comparing different MR valve configurations using analytical models and Finite Element Analysis [FEA] [10]. This type of analysis is remarkably time consuming with various processes involved in the evaluation to determine the most suitable design for a particular application. In order to shorten the process, this study aims to compare the pressure drop generated by each types of MR valves. The operating range and the pressure magnitude are also discussed. Thus, the analysis serves as a basis in selecting or designing tool for MR valves.

2 MR valve modelling

The performance of an MR valve is analyzed here based on its capability in producing and flexibility in pressure drop between upstream and downstream sides. Valve ratings are mainly determined by the pressure drop hence the expression of mathematical modelling of pressure drop for each configuration in each section. The basic expression of the pressure drop in the MR valve is observed as [11]:

$$\Delta P = \Delta P_{\text{Viscous}} + \Delta P_{\text{Yield}} \tag{1}$$

where $\Delta P_{\text{Viscous}}$ and ΔP_{Yield} are the viscous and field dependent yield stress of pressure drop. The mathematical expression of viscous and field dependent pressure drop for annular and radial flow path is observed as in Table 1 [12] :

Table 1. Mathematical equations.

	Viscous ($\Delta P_{\text{Viscous}}$)	**Yield** (ΔP_{Yield})
Annular	$\frac{6\eta QL}{\pi d^3 R}$. (2)	$\frac{c\tau\,(B)L}{d}$, (3)
Radial	$\frac{6\eta\,Q}{\pi d^3}\text{In}\left(\frac{R_0}{R_i}\right)$, (4)	$\frac{c\tau\,(B)}{d}(R_0 - R_i)$, (5)

where d is the valve gap, η is the fluid base viscosity, Q is the flow rate, L is the annular channel length of the valve, R is the channel radius, $\tau(B)$ is the field dependent yield stress value and c is the flow velocity profile coefficient. Also the valve gap size d in equations refers to radial gaps while R_0 and R_i referring to the inner radial gaps and outer radius of radial gaps respectively.

The coefficient of c can be obtained through the calculation of ratio between viscous pressure drop and the total pressure drop as seen following:

$$c = 2.07 + \frac{12Q\eta}{12Q\eta + 0.8\pi R d^2 \tau\,(B)}. \tag{6}$$

Meanwhile, for the equation on the orifice gaps, the expression is slightly different since there is no field dependent yield stress on the MR fluid. The pressure drop equation of orifice gaps solely expressed in viscous resistance as shown [13]:

$$\Delta P = 2\frac{8\eta QL}{\pi R^4} \tag{7}$$

3 MR valve configurations

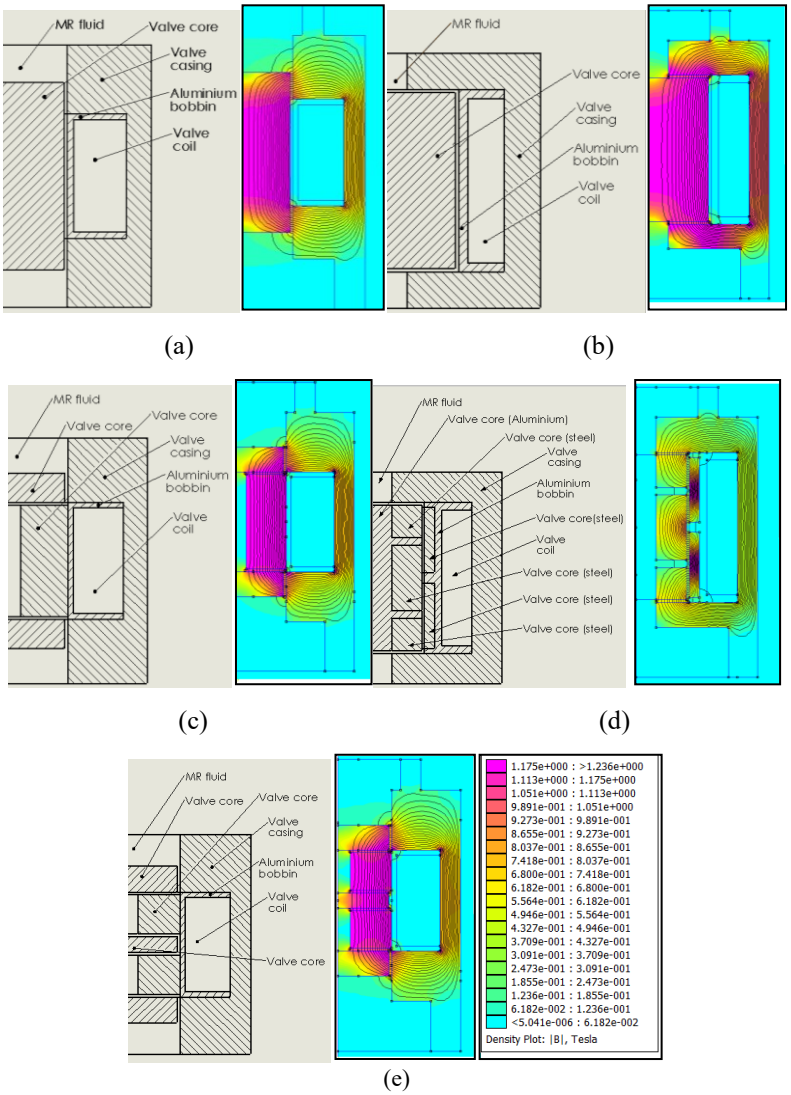

Fig. 1. Configuration of MR valve in FEMM simulation (a) annular, (b) radial, (c) annular-radial, (d) serpentine (e) meandering

In this research paper, the strength of magnetic flux densities was evaluated to predict the performance of MR valve as shown in Figure 1. The magnetic field strength of MR valves

are difficult to measure through experimental method thus why the numerical approach was chosen to aid the prediction of MR effect that will be generated by the MR fluid. The author chose the FEMM (Finite Element Method Magnetics) software to analyze magnetic simulations in this study.

Parameters are required when conducting the simulation to obtain the magnetic flux distributions. The coils of each MR valve were designed and fixed with 450 turns of 24 AWG copper wires and a total resistance of 5.5 Ω. Due to the maximum current applied to the coil being 1 A, the power consumption is only 5.5 watt. The simulation was conducted in 2D axis-symmetric with different total elements and node according to the type of MR valves. The permeability of MR fluid was obtained from the manufacturer. The permeability of magnetic material of MR valve is assumed to be similar to the B-H curve of AISI 1020 while the permeability of non-magnetic is assumed to be the B-H curve of AISI 6061-T6. The results will be discussed in each section for each type of MR valve.

4 Pressure drop generated by MR valve

Figure 2 depicts the pressure drop versus current for the MR valve that was proposed in this study. The figure shows the MR valve could experience various pressure drop under different types of configurations because of the effect of the magnetic field intensity that was generated by the coils. During the off-state, the MR valve would work based on the viscosity of the MR fluid like the existing damper. It was identified that the serpentine MR valve can produce a damping force of 0.06 MPa in the absence of the input current and could increase up to 4.4 MPa by applying the input current of 1.0 A. Meanwhile the meandering configuration was able to produce damping force of 0.07 MPa and with the presence of 1.0 A, the range increases up to 3.6 MPa. Specifically, these two configurations portrayed the highest damping force produced by the five MR valve configurations.

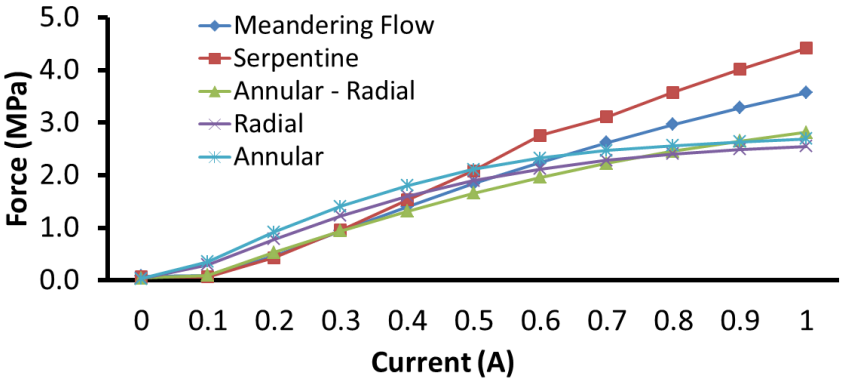

Fig. 2. Pressure drop comparison

Figure 3 depicts the off-state pressure drop generated by each MR valves. The figure shows meandering having the highest force and annular the lowest. Meanwhile, Figure 4 shows the on-state pressure drop generated. Serpentine configuration produced the highest while meandering the second highest in pressure drop generation.

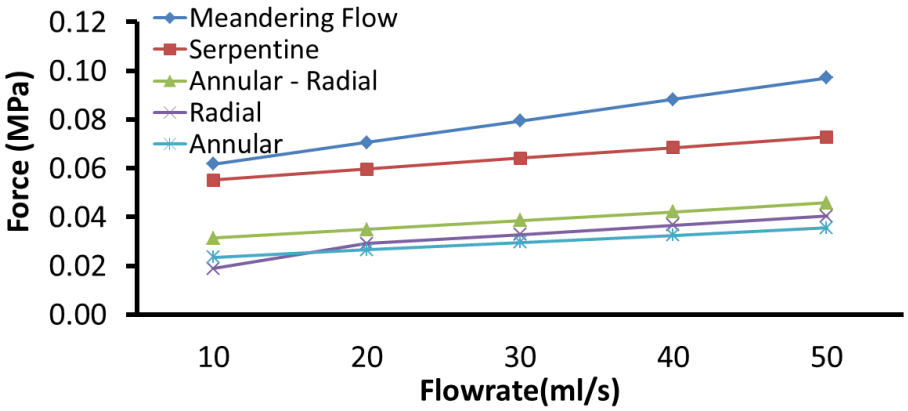

Fig. 3. Off-state pressure drop of MR valve

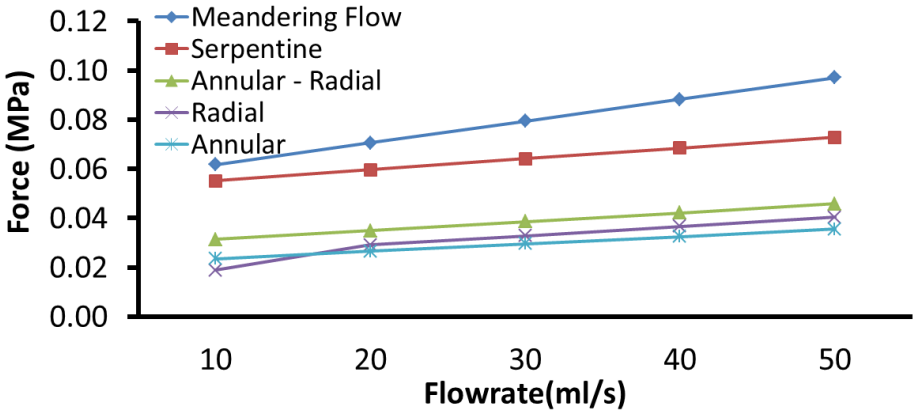

Fig. 4. On-state pressure drop of MR valve

Figure 5 illustrates the widest range of the pressure drop generated from each type of MR valves. Serpentine produced the biggest value compared to the other MR valves. The meandering valve ranked the second highest in pressure drop generated followed by annular-radial. The lowest falls to radial and is followed by the annular configurations.

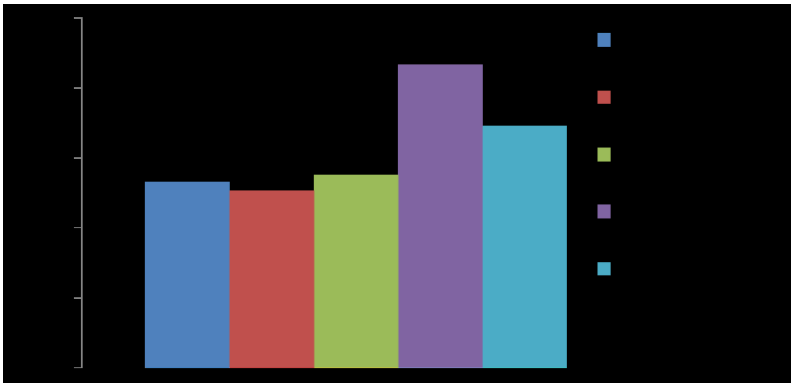

Fig. 5. Dynamic range of MR valve

5 Conclusion

The presented study discussed the comparison of five different types of MR valve: annular, radial, annular-radial, serpentine and meandering valves. For each type of MR valves, individual mathematical modelling of pressure drop for each type of MR valves were developed and the results were compared. The proposed approach aims to study the different configuration of MR valves' performances. The analysis also considers the same size of MR valves, gap size, number of turns and power consumption.

This research was financially supported by the Universitas Sebelas Maret (UNS) through Hibah Kolaborasi Internasional 2017 and Universiti Teknologi Malaysia under PRGS Grant (Vote No: 4L667) and Tier 1 Grant (Vote No: 13H55).

References

1. P.P. Phulé, Smart Mater. Bull. **2001**, 7, (2001).
2. F. Imaduddin, S.A. Mazlan, H. Zamzuri, M.A.A. Rahman, Appl. Mech. Mater. **663**, 685, (2014).
3. A.Y. Abd Fatah, S.A. Mazlan, T. Koga, H. Zamzuri, F. Imaduddin, Int. J. Appl. Electromagn. Mech. **50,** 29, (2016).
4. X. Bai, N.M. Wereley, Y. Choi, J. Intell. Mater. Syst. Struct. **27,** 944, (2016).
5. H. Sahin, F. Gordaninejad, X. Wang, Y. Liu, J. Intell. Mater. Syst. Struct. **23**, 949, (2012).
6. H. Hu, X. Jiang, J. Wang, Y. Li, J. Intell. Mater. Syst. Struct. **23**, 635, (2012).
7. A.Z. Bin Pokaad, K. Hudha, M.Z.B.M. Nasir, N.A. Ubaidillah, Int. J. Struct. Eng. **2,** 164, (2011).
8. F. Gordaninejad, X. Wang, G. Hitchcock, K. Bangrakulur, S. Ruan, M. Siino, J. Struct. Eng. **136,** 135, (2010).
9. F. Imaduddin, S.A. Mazlan, H. Zamzuri, M.A.A. Rahman, Ubaidillah, B. Ichwan, Smart Mater. Struct. **23,** 065017**,** (2014).
10. T. Xu, M. Liang, C. Li, S. Yang, J. Sound Vib. **355,** 66, (2015).
11. H.X. Ai, J. Intell. Mater. Syst. Struct. **17,** 327, (2006).
12. Q.-H. Nguyen, S.-B. Choi, N.M. Wereley, Smart Mater. Struct. **17,** 025024, (2008).
13. A. Grunwald, A.G. Olabi, Sensors Actuators, A Phys. **148**, 211, (2008)